Solution Nonideality Related to Solute Molecular Characteristics of Amino Acids

Carl R. Keener, Gary D. Fullerton, Ivan L. Cameron, and Jinhu Xiong
Departments of Radiology and Cellular and Structural Biology, University of Texas Health Science Center at San Antonio, San Antonio, Texas 78284-7800 USA

ABSTRACT By measuring the freezing-point depression for dilute, aqueous solutions of all water-soluble amino acids, we test the hypothesis that nonideality in aqueous solutions is due to solute-induced water structuring near hydrophobic surfaces and solute-induced water destructuring in the dipolar electric fields generated by the solute. Nonideality is expressed with a single solute/solvent interaction parameter I, calculated from experimental measure of ΔT. A related parameter, I_n, gives a method of directly relating solute characteristics to solute-induced water structuring or destructuring. I_n-values correlate directly with hydrophobic surface area and inversely with dipolar strength. By comparing the nonideality of amino acids with progressively larger hydrophobic side chains, structuring is shown to increase with hydrophobic surface area at a rate of one perturbed water molecule per 8.8 square angstroms, implying monolayer coverage. Destructuring is attributed to dielectric realignment as described by the Debye-Hückel theory, but with a constant separation of charges in the amino-carboxyl dipole. By using dimers and trimers of glycine and alanine, this destructuring is shown to increase with increasing dipole strength using increased separation of fixed dipolar charges. The capacity to predict nonideal solution behavior on the basis of amino acid characteristics will permit prediction of free energy of transfer to water, which may help predict the energetics of folding and unfolding of proteins based on the characteristics of constituent amino acids.

INTRODUCTION

Presently, no methods exist that can relate nonideal colligative properties of solutions to solute molecule characteristics. A new set of empirical equations describing freezing-point depression, osmotic pressure, and vapor pressure make it possible to address this problem (Fullerton et al., 1992; Zimmerman et al., 1993). The solute/solvent interaction equations isolate the description of nonideality in terms of a single constant, I, for a given solute; they were derived by trivial substitution of the corrected solvent mass for the actual solvent mass:

$$M_w^c = M_w - I \cdot M_s. \quad (1)$$

For example, the nonideal but accurate linear equation for freezing-point depression,

$$\frac{M_w}{M_s} = \frac{k_f \cdot 1000}{A_e} \times \frac{1}{\Delta T} + I, \quad (2)$$

replaces the ideal, but inaccurate, equation

$$\Delta T = k_f \times \frac{1000}{A_s} \times \frac{M_s}{M_w}, \quad (3)$$

where

M_w^c = mass of water in grams (corrected for nonideality),
M_w = mass of water in grams,
M_s = mass of solute in grams,
k_f = freezing-point depression constant for water (1.858°C/mol),
A_e = colligative effective mulecular weight (experimentally measured),
A_s = chemical molecular weight,
ΔT = solution freezing-point depression in °C, and
I = (mass perturbed water)/(mass solute) = nonideality parameter.

Foundations of the interaction-corrected (IC) hypothesis

Recent literature concerning nonideal solutions proposes a number of methods for dealing with nonideality. In the study of proteins, Arakawa and Timasheff use the concepts of preferential hydration (Arakawa et al., 1990a, b; Arakawa and Timasheff, 1984), whereas Minton uses the concept of volume occupancy by the solute, which leads to predictions of molecular crowding (Minton, 1983a, b; Minton and Edelhoch, 1982). Simultaneously, Parsegian and his colleagues developed the concepts of hydration force due to layers of perturbed solvent extending multiple layers from a variety of molecular surfaces including polar lipid membranes, nucleotide polymers, and proteins (LeNeveu et al., 1977; LeNeveu et al., 1976; Parsegian et al., 1986; Parsegian, 1967; Prouty et al., 1985). On the other hand, growing experience with molecular dynamics is providing evidence that solvent perturbations occur at molecular surfaces (Rossky and Karplus, 1979; Sonnenschein and Heinzinger, 1983; Marchesi, 1983; Geiger, 1981; Marlow et al., 1993). In addition, solvent motion and structure changes adjacent to solute molecules have been experimentally confirmed by NMR (Fullerton et al., 1986; Grosch and Noack, 1976; Zimmerman et al., 1985; Hertz, 1973), as well as by x-ray and neutron diffraction measurements (Finney and Turner, 1986; Soper

Received for publication 13 June 1994 and in final form 9 September 1994.
Address reprint requests to Dr. Gary D. Fullerton, Department of Radiology, University of Texas Health Science Center, 7703 Floyd Curl Drive, San Antonio, TX 78284-7800. Tel.: 210-567-5550; Fax: 210-567-5549.

0006-3495/95/01/291/12 $2.00

et al., 1977; Enderby and Neilson, 1980; Enderby and Neilson, 1981). It is our belief that all of the above alternative approaches are correct descriptions of solute/solvent interface effects. This study uses the interaction-corrected method of modifying thermodynamic expressions, which was first presented as a set of empirical equations (Fullerton et al., 1992, 1993; Kanal et al., 1994). This method was recently more rigorously related to the existing body of thermodynamic knowledge (Fullerton et al., 1994).

Derivation of the IC equations

The textbook approach to dealing with nonideality, as proposed by Lewis and Randall (Harned and Owen, 1950; Levine, 1988), shows that the chemical potential of a solute is expressed as

$$\mu_s = \mu_s^0 + RT \ln a_s = \mu_s^0 + RT \ln \gamma_s x_s, \qquad (4)$$

where

μ_s = chemical potential of the solute,
μ_s^0 = reference chemical potential,
R = universal gas constant,
T = absolute temperature,
a_s = solute activity,
γ_s = solute activity coefficient, and
x_s = solute mole fraction.

In Fig. 1, we plot the activity of a typical solution for which $\gamma > 1$ in comparison to the ideal solute for which $\gamma = 1$. It is clear from this plot that equivalent activities a' occur at very different concentrations or mole fractions for real and ideal solutes such that

$$a_s = \gamma_s x_s = x_s^{id} \qquad (5)$$

where x_s^{id} = mole fraction of an ideal solute. A virial expansion is traditionally used to describe γ. However, unlike I, the virial expansion has no underlying theoretical explanation.

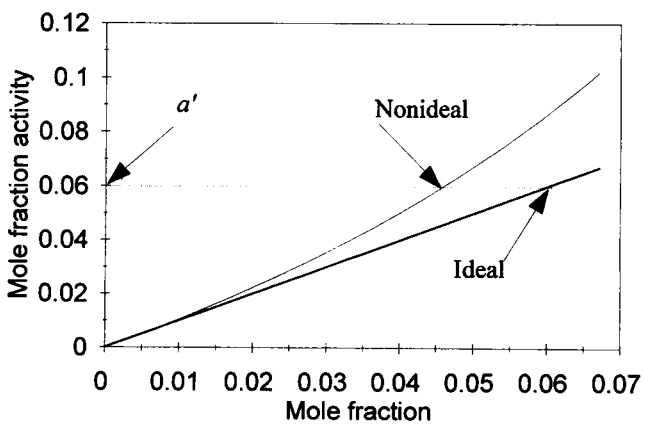

FIGURE 1 A conceptual diagram demonstrates the relation of the mole fraction activity of a real, or nonideal, solution relative to an ideal solution. The thermodynamic activity of the solute, a', is equivalent for solutions of quite different mole fraction content—x_s for the real solute and x_s^{id} for the ideal solute. Using the solute/solvent interaction hypothesis, this difference is assigned to perturbed solvent adjacent to the solute molecule such that correct free water mass is reduced by a fixed amount per solute molecule such that

$$a' = \gamma_s x_s = x_s^{id} = \frac{M_s/A_s}{(M_w - IM_s)/A_w + M_s/A_s}.$$

It is at this point that we apply the solute/solvent interaction hypothesis suggested by molecular dynamics simulations and modern studies of solvent structure as noted above. We assume that each solute molecule perturbs the solvent by an equivalent amount such that the interaction-corrected solvent mass is shown by Eq. 1. We emphasize that the solute/solvent interaction coefficient is a molecular concept quite independent of thermodynamics. It is suggested by surface effects on each solute molecule that

$$I_n = \frac{N_w^p}{N_s} = \frac{\text{number of perturbed water molecules}}{\text{per solute molecule}}, \qquad (6)$$

where

N_w^p = number of perturbed water molecules in solution, and
N_s = number of solute molecules in solution,

which is easily converted to relative masses if the molar masses are known.

$$I = I_n \cdot \frac{A_{water}}{A_{solute}}, \qquad A = \text{molar mass}. \qquad (7)$$

If the nonideality parameter I is a measure of solute/solvent interaction, as we have previously suggested (Fullerton et al., 1994), then it provides a method to directly relate solute characteristics to solute-induced solvent structuring or destructuring. The purpose of this study is to test this hypothesis and to show that the nonideality parameter (I) directly measures water structuring changes near the surface of the solute molecule. We will also show that these water-structuring changes can be correlated to solute molecular characteristics by using I_n, which describes nonideality per solute *particle* rather than solute *mass*. This study shows that nonideality is the summation of several interface effects that are predictable on the basis of solute characteristics: solvent-accessible hydrophobic surface area, hydrophilic charge geometry, and molecular weight.

MATERIALS AND METHODS

Materials

Glycine, L-alanine, L-valine, L-leucine, L-isoleucine, L-proline, L-methionine, L-phenylalanine, L-lysine, L-arginine, DL-serine, L-threonine, L-cysteine, L-asparagine monohydrate, L-glutamine, L-histidine, diglycine, triglycine, di-DL-alanine and tri-L-alanine were purchased from Sigma Chemical Co. (St. Louis, MO) in the purest form readily available (Sigma grade, purity > 99% TLC). Sample solutions were prepared without further purification.

Solutes are grouped into three general classifications—hydrophobic, hydrophilic, and peptides—and then subclassified based on molecular characteristics (DeRobertis and DeRobertis, 1980). The hydrophobics consist of amino acids with aliphatic hydrocarbon side chains (glycine, alanine, valine, isoleucine, and leucine) and those with nonaliphatic or nonhydrocarbon side chains: proline (heterocyclic), phenylalanine (aromatic), methionine (sulfur-containing). The hydrophilics were subdivided into polar and ionic, the ionic

having ionized side chains at physiological pH. The polar hydrophilics include cysteine (sulfur-containing), serine and threonine (hydroxyl-containing), asparagine and glutamine (amide-containing), histidine and tryptophan (heterocyclic), and tyrosine (aromatic). The ionic hydrophilics include lysine and arginine (both basic) plus glutamic acid and aspartic acid (both acidic). The peptides consist of polymers of glycine and polymers of alanine. Table 1 lists the solutes used in this experiment along with their pertinent molecular characteristics.

Methods

We chose to test all of the amino acids at similar concentrations. Because many are only slightly soluble in water, 0.2 M was the maximum concentration used. This concentration is sufficient to produce low uncertainty in measurements, yet dilute enough to prevent overlapping of hydration layers of adjacent solute molecules. The validity of the interaction-corrected formula for freezing-point depression has been previously demonstrated to extend from this low concentration through a high concentration of 2–3 M for glucose, sucrose, ethylene glycol, and glycerol (Fullerton et al., 1994). The 0.2 M solutions were prepared for each solute by adding approximately 50 g of deionized, degassed water to the appropriate mass of solute. Solutions containing less-soluble solutes (phenylalanine and leucine) were filtered with 0.45 μm Acrodisc syringe filters. Amino acids that were too insoluble to produce 0.2 M solutions (tryptophan, tyrosine, glutamic acid, aspartic acid) were not used. Each solution was then measured by volume into five glass vials and diluted to produce five concentrations ranging from 0.1 to 0.2 M.

The freezing point was measured using an Osmomat 030 freezing-point osmometer (UIC, Joliet, IL). For each experiment, five concentrations were sampled four times. A small aliquot was placed in a microfuge tube that was then super-cooled to −6.87°C by the osmometer with a built-in Peltier cooling system. A crystallization needle was injected into the sample, and a thermistor probe measured the crystallization temperature. After approximately 2 min, the osmometer digitally displayed the ideal osmolality in Osm/kg. The change in freezing point (ΔT) was calculated as $\Delta T = k_f \times$ *reading*, using the mean of the four readings. The measurement error for the Osmomat 030 at these concentrations is 1%.

Concentrations were determined gravitmetrically by freeze-drying followed by vacuum heating; the two techniques were used in combination to ensure the removal of all residual moisture without damaging the solute molecules. Using 1 g aluminum weighing dishes, approximately 10 ml of each concentration was frozen on dry ice and then freeze-dried overnight in a glass dessicator with a 1L Labconco Dry-ice Freeze-dry System (Labconco, Kansas City, MO). The samples were back-filled with dry nitrogen and then vacuum-dried overnight at 60°C. The samples were again back-filled with nitrogen and weighed. The mass of water was calculated by subtracting the residual mass from the solution mass, and the solute mass was determined by subtracting the mass of the weighing dish from the residual mass. The ratio of mass water to mass solute (M_w/M_s) was calculated using the mass water (g)/mass amino acid (g) ratio.

The drydown technique was tested using a solution of a known mass of glycine in a known mass of water. The average difference between the known and measured M_w/M_s was −0.51 and −0.81%, respectively, in two experiments of five samples each.

TABLE 1 Characteristics of the solutes used in this study

		Side chain characteristic	Water solubility g/100 ml H_2O at 25°C	A_s	Side-chain *ASA* (Å^2)	
					Nonpolar area	Polar area
Hydrophobic (aliphatic hydrocarbon)						
Glycine	Gly	alipathic	25.0	75.0	0	0
Alanine	Ala	aliphatic	16.7	89.1	67	0
Valine	Val	aliphatic	8.9	117.1	117	0
Isoleucine	Ile	aliphatic	4.1	131.2	140	0
Leucine	Leu	aliphatic	2.4	131.2	137	0
Hydrophobic (other)						
Proline	Pro	heterocyclic	162.0	115.1	105	0
Phenylalanine	Phe	aromatic	3.0	165.2	175	0
Methionine	Met	sulfur	3.4	149.2	117	43
Hydrophilic (polar)						
Cysteine	Cys	sulfur	very	121.2	35	69
Serine	Ser	hydroxyl	5.0	105.1	44	36
Threonine	Thr	hydroxyl	20.5	119.1	74	28
Asparagine	Asn	amide	15.0	132.1	44	69
Glutamine	Gln	amide	3.7	146.1	53	49
Histidine	His	heterocyclic	4.2	155.2	102	49
Tryptophan	Trp	heterocyclic	1.14	204.2	190	27
Tyrosine	Tyr	aromatic	0.04	181.2	144	43
Hydrophilic (ionic)						
Lysine	Lys	basic	very	146.2	119	48
Arginine	Arg	basic	15.0	174.2	89	107
Glutamic acid	Glu	acidic	0.86	147.1	61	77
Aspartic acid	Asp	acidic	0.50	133.1	48	58
Peptides						
Diglycine	2Gly	polyglycine		132.1	0	0
Triglycine	3Gly	polyglycine		189.2	0	0
Dialanine	2Ala	polyalanine		160.2	134	0
Trialanine	3Ala	polyalanine		231.3	201	0

The solutes were divided into hydrophobic amino acids, hydrophilic amino acids, and peptides and then further classified based on the side-chain, molecular characteristics as shown in this table (DeRobertis and DeRobertis, 1980). The four amino acids shown in italics are too insoluble for inclusion in this study (Streitweiser and Heathcock, 1981; Weast, 1981). The chemical weights are from the manufacturer and the CRC handbook (Weast, 1981). The side-chain solvent-accessible surface areas (*ASA*) were calculated by Miller using the rolling ball method (Miller et al., 1987). The side-chain *ASA* for the peptides is the sum of the side-chain *ASA* of the constituent residues.

The above experimental procedure was repeated 3 times for each amino acid. The inverse of the concentration (M_w/M_s) was plotted against the inverse of the freezing-point depression ($1/\Delta T$), and the line of best fit was calculated by linear regression. The effective molecular weight was calculated from the slope (S) of the regression line where $A_e = k_f \times 1000/S$. The interaction parameter (I) was then calculated for each measurement using the relationship

$$I = \frac{M_w}{M_s} - \frac{1000 \cdot k_f}{A_s} \times \frac{1}{\Delta T}, \quad (8)$$

where the effective molecular weight (A_e) has been replaced with the chemical molecular weight (A_s) after showing that $A_e \approx A_s$. This demonstrates sample purity and the accuracy of the molecular weight for each measurement, allowing all deviations in ΔT to be attributed to I. The data were combined to calculate a mean I-value with a 95% confidence interval (t-interval). To reduce the propagation of random error due to increased measurement uncertainties at low concentrations, data with $1/\Delta T > 5.2$ were not accepted. This was repeated for each amino acid, and a one-way ANOVA was performed to demonstrate statistically significant differences in the I-values among the amino acids tested. The Student-Neuman-Keuls (SNK) multiple range test was then used to determine which I-values were different at the $p = 0.05$ level of significance. Statistical analysis was performed with Quattro Pro and SSPS computer programs.

RESULTS

The results of three experiments with glutamine are presented as a representative example of the treatment of each of the 20 amino acids and peptides. Table 2 shows the data from the three experiments. Fig. 2 *a*, a traditional plot of ΔT versus concentration, shows that the experimental data have a negative deviation from ideal as calculated by Eq. 3. Fig. 2 *c*, an inverse plot of M_w/M_s vs. $1/\Delta T$, shows that the negative I deviation is constant over the range of concentrations tested. The slope of the regression line of the experimental data yields an effective molecular weight of A_e = 146.4, a difference of 0.22% from the chemical molecular weight. Table 2 and Fig. 2, *b* and *d* also show the results for leucine, which has a positive deviation from ideal. The slope of the regression line of the experimental data for leucine yields an effective molecular weight of A_e = 132.0, a difference of 0.63% from the chemical molecular weight.

TABLE 2 Experimental data for glutamine and leucine

Glutamine					
Experiment	ΔT	M_s/M_w	$1/\Delta T$	M_w/M_s	I
A	0.202	0.0161	4.960	61.98	−1.101
A	0.235	0.0187	4.263	53.38	−0.840
A	0.268	0.0215	3.731	46.47	−0.978
A	0.303	0.0245	3.297	40.74	−1.185
A	0.333	0.0269	3.003	37.11	−1.071
B	0.196	0.0157	5.114	63.51	−1.518
B	0.229	0.0183	4.358	54.52	−0.897
B	0.264	0.0212	3.784	47.21	−0.908
B	0.297	0.0240	3.364	41.58	−1.198
B	0.327	0.0264	3.054	37.85	−0.983
C	0.199	0.0159	5.030	62.70	−1.268
C	0.231	0.0185	4.323	54.13	−0.845
C	0.261	0.0213	3.838	47.01	−1.798
C	0.298	0.0241	3.359	41.41	−1.298
C	0.328	0.0267	3.045	37.50	−1.220
				I(mean) = −1.14 ± 0.15	
Leucine					
Experiment	ΔT	M_s/M_w	$1/\Delta T$	M_w/M_s	I
A*	0.174	0.0121	5.741	82.709	1.408
A	0.203	0.0140	4.938	71.446	1.519
A	0.231	0.0160	4.323	62.354	1.134
A	0.257	0.0177	3.893	56.587	1.456
A	0.294	0.0200	3.406	49.927	1.687
B*	0.165	0.0114	6.047	87.357	1.718
B	0.193	0.0134	5.188	74.743	1.278
B	0.221	0.0153	4.532	65.522	1.337
B	0.252	0.0174	3.972	57.545	1.295
B	0.280	0.0193	3.570	51.899	1.339
C*	0.143	0.0098	7.013	101.882	2.573
C*	0.168	0.0115	5.964	86.753	2.299
C*	0.190	0.0130	5.277	76.805	2.080
C	0.214	0.0148	4.670	67.694	1.560
C	0.241	0.0164	4.156	60.938	2.081
				I(mean) = +1.47 ± 0.19	

Three experiments (A, B, and C) were performed on each. The freezing-point depression (ΔT) and concentration (M_s/M_w) were measured for five concentrations in each experiment. The inverses of those measurements ($1/\Delta T$ and M_w/M_s) were used to calculate the interaction parameter (I) using Eq. 8.

*To reduce measurement uncertainty, we did not accept data points with $1/\Delta T > 5.2$.

The other 18 samples were treated similarly. The purity of the samples and effectiveness of the experimental technique are shown in Table 3 and Fig. 3, which plots the effective molecular weight (A_e) versus the chemical molecular weight (A_s). Only the hydrophilic ionic molecules showed a large deviation between A_e and A_s. The difference between A_e and A_s (ΔA) in the initial experiments for lysine, arginine, and asparagine was 9.2, 12.6, and −4.8%, respectively. Because each has a high affinity for water (lysine and arginine are charged molecules, lysine is hygroscopic, and asparagine is supplied as a monohydrate), it was hypothesized that 60°C was not sufficient to completely dry these three amino acids. The large error for the ionic solutes (lysine and arginine) is also thought to be due to uncertainty concerning side-chain ionic dissociation. Therefore, these samples were heated at progressively higher intervals of approximately 10°C and weighed after each heating to observe a temperature plateau at which all the water was removed without decomposing the sample. For asparagine, the ideal temperature was found to be 100°C. The experiments for asparagine were repeated with this drydown temperature resulting in an acceptable $\Delta A = -1.81\%$. This temperature was subsequently used for the hygroscopic peptides. The samples of lysine and arginine continued to decrease in mass and discolor with higher temperatures, indicating that increased heating was decomposing the samples without removing all of the remaining water. Because of these difficulties, the data from the two ionic amino acids are not included in the molecular weight statistical analysis.

The RMS error of A_e for the 18 nonionic solutes is 1.81%. Regression analysis of A_e vs. A_s yields a slope of 0.994, and a correlation coefficient of r = 0.997 with 16 degrees of

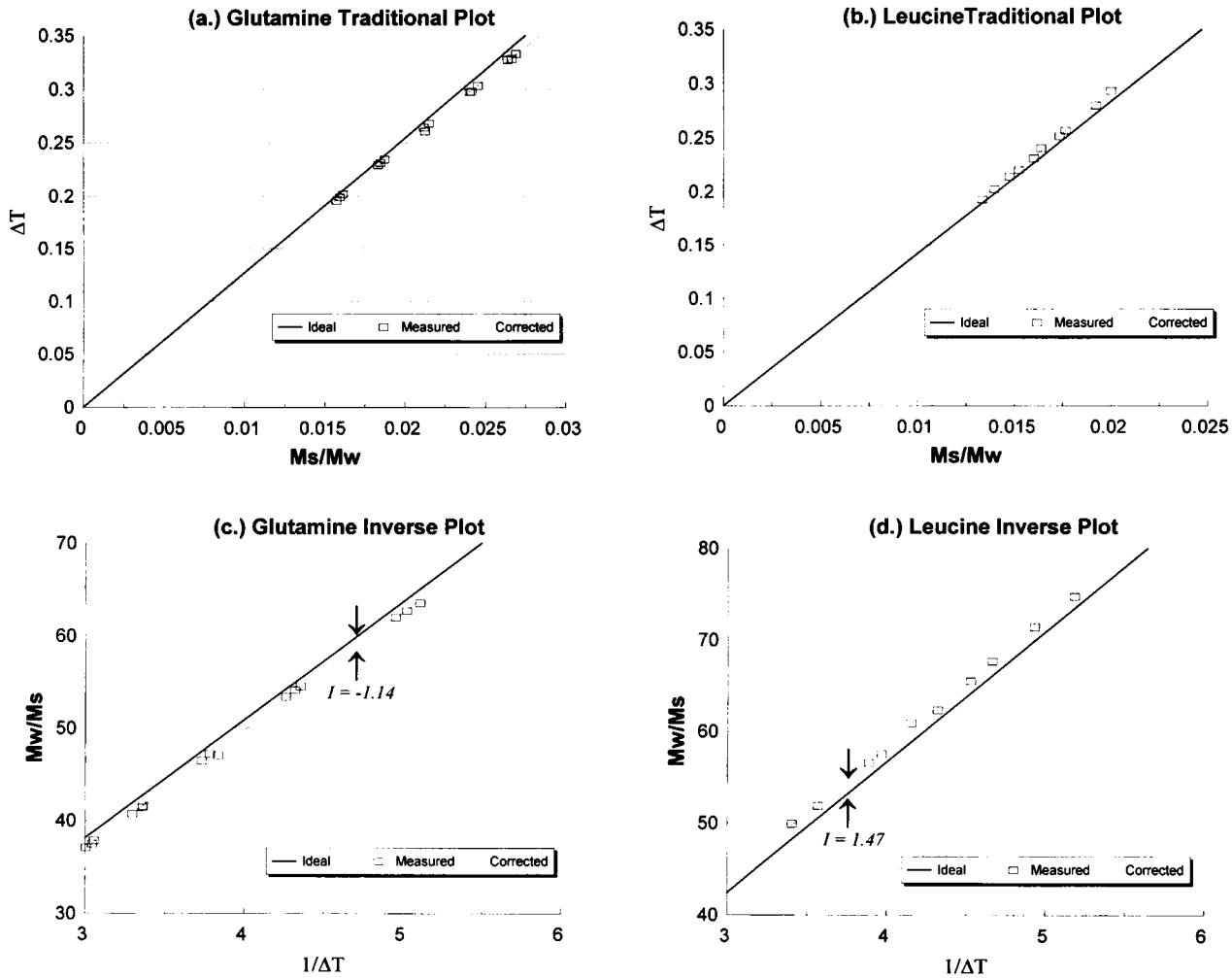

FIGURE 2 Plots of the freezing-point depression data of glutamine and leucine. (*a*) Solutions of glutamine have a negative deviation from ideal, whereas (*b*) solutions of leucine have a positive deviation from ideal. (*c*) The same glutamine data in the interaction-corrected inverse plot (inverse of concentration versus inverse freezing-point depression) shows the deviation as a constant negative 1.14 g of water per gram of glutamine (for this range of concentrations). Fullerton et al. have shown that this value (*I*) can be used to correct the mass of water in solution for the recalculation of ΔT that matches the experimental data (Zimmerman et al., 1993; Fullerton et al., 1992):

$$\Delta T = \frac{1000 \times k_f}{A_s} \times \frac{1}{(M_w/M_s) - I}.$$

(*d*) The same leucine data in an inverse plot shows that the deviation is a constant positive 1.47 g of water per gram of leucine (for this range of concentrations).

freedom. There is not a statistically significant difference between A_e and A_s. We therefore substitute $A_s = A_e$ and assign all variation from ideal to the *I*-value.

An *I*-value was calculated for each data point using Eq. 8. Table 2 shows the *I*-value for each measurement of glutamine and leucine. For glutamine, the mean *I*-value is -1.14 (g water/g glutamine) with a 95% confidence interval of 0.15. Therefore, the freezing-point depression of glutamine shows a constant deviation from ideal of $I = -1.14 \pm 0.15$ (g water/g glutamine), as shown in Fig. 2 *c* and summarized in Table 4. For leucine, the mean *I*-value of the 10 acceptable measurements is 1.47 (g water/g leucine) with a 95% confidence interval of 0.19. Therefore, the freezing-point depression of leucine shows a constant deviation from ideal of $I = 1.47 \pm 0.19$ (g water/g leucine).

The deviations from ideal for all 20 samples are shown in Table 4. *I*-values express nonideality in terms of (mass of perturbed water/mass of solute). I_n-values express nonideality in terms of (number of perturbed water molecules/solute molecule)

$$I_n = I \times \frac{A_{solute}}{A_{water}}, \qquad A = \text{molecular weight.} \quad (9)$$

I is measured experimentally; in Results, we refer to *I*-values and their statistical analysis. I_n is more useful in visualizing the water perturbation per solute particle; in Discussion, we refer to I_n-values and their statistical analysis. The I_n-values for the 16 tested amino acids are plotted with their 95% confidence intervals in Fig. 4.

TABLE 3 Effective molecular weight and RMS error

	Chemical molecular weight (A_s)	Number of samples (n)	Effective molecular weight (A_e)	Molecular weight error (ΔA)
Hydrophobic (aliphatic hydrocarbon)				
Glycine	75.0	13	74.3	-0.91%
Alanine	89.1	15	86.3	-3.12%
Valine	117.1	15	115.0	-1.78%
Isoleucine	131.2	15	128.0	-2.42%
Leucine	131.2	10	132.0	0.63%
Hydrophobic (other)				
Proline	115.1	12	115.7	0.55%
Phenylalanine	165.2	14	159.5	-3.42%
Methionine	149.2	15	150.7	0.98%
Hydrophilic (polar)				
Cysteine	121.2	15	117.7	-2.87%
Serine	105.1	15	103.5	-1.49%
Threonine	119.1	15	118.3	-0.66%
Asparagine	132.1	15	129.7	-1.81%
Glutamine	146.1	15	146.4	0.22%
Histidine	155.2	15	156.6	0.92%
Hydrophilic (ionic)				
Lysine	146.2	14	159.6	9.15%
Arginine	174.2	14	203.3	16.69%
Peptides				
Diglycine	132.1	15	129.1	-2.30%
Triglycine	189.2	15	187.0	-1.15%
Dialanine	160.2	10	157.3	-1.79%
Trialanine	231.3	5	229.2	-0.92%
RMS error (nonionic solutes) =				1.81%
RMS error (all solutes) =				4.59%

The effective molecular weight (A_e) of each solute was calculated from the slope (S) of the regression line using the equation $A_e = k_f \times 1000/S$. The RMS error is a good estimate of the accuracy of measuring the molecular weight of small nonionic solutes using freezing-point depression data.

Statistical analysis of *I*

All of the hydrophilic amino acids have negative deviations from ideal. All of the hydrophobic amino acids, except glycine and phenylalanine, have positive deviations from ideal. One-way ANOVA shows that the difference in the I-values is highly significant ($p \ll 0.001$). The SNK multiple range test shows that all the negative I-values are different from the positive I-values at the $p = 0.05$ level of significance.

For hydrophobic amino acids, the deviations from ideal range from $I = -1.01$ for glycine to $I = 2.03$ for proline. This is a highly significant difference ($p \ll 0.001$), and each I-value is significantly different ($p < 0.05$) from at least six others in this group of eight. For hydrophilic polar amino acids, the deviations from ideal range from $I = -2.08$ for serine to $I = -0.10$ for cysteine. This difference is also highly significant ($p \ll 0.001$), and each I-value is significantly different ($p \ll 0.05$) from at least four others in this group of six.

Peptides of glycine have deviations ranging from $I = -2.58$ for triglycine to $I = -1.01$ for glycine. The difference is highly significant ($p \ll 0.001$), and the I-values in this group are all significantly different ($p < 0.05$) from each other. Peptides of polyalanine have deviations ranging from $I = 0.82$ for dialanine to $I = 1.44$ for trialanine. The difference in this group is less significant ($p < 0.10$) than in the other groups, partially because of the smaller sample sizes of these peptides.

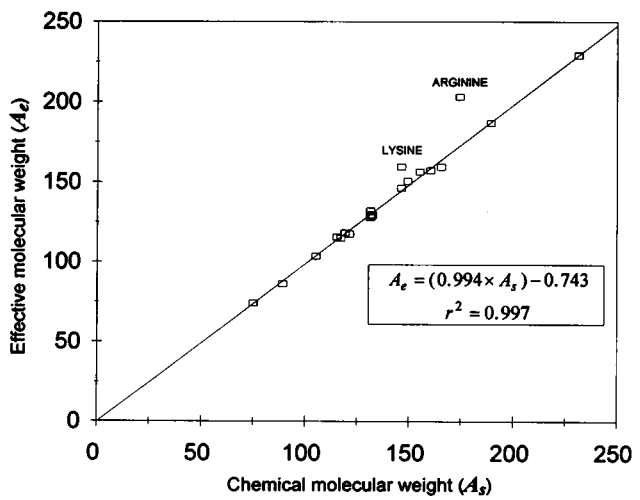

FIGURE 3 Plot of the experimentally measured effective molecular weight (A_e) versus chemical molecular weight (A_s) of all solutes measured. The regression line includes all of the solutes except lysine and arginine, whose molecular weights could not be accurately measured. The data points have a very close fit to a line with nearly unity slope, indicating the purity of the solutes and the accuracy of the experimental technique. On this basis, we accept substitution of $A_s = A_e$ and assign all error to the experimental measurement of I.

TABLE 4 Nonideality with 95% confidence intervals for each of the 16 amino acids and 4 peptides measured

	Side-chain characteristic	I-value $\left(\frac{\text{mass water}}{\text{mass solute}}\right)$	I_n-value $\left(\frac{\text{water molecules}}{\text{solute molecule}}\right)$
Hydrophobic (aliphatic hydrocarbon)			
Glycine	aliphatic	-1.01 ± 0.19	-4.22 ± 0.81
Alanine	aliphatic	1.10 ± 0.36	5.47 ± 1.78
Valine	aliphatic	1.52 ± 0.16	9.91 ± 1.07
Isoleucine	aliphatic	1.78 ± 0.20	12.98 ± 1.49
Leucine	aliphatic	1.47 ± 0.19	10.70 ± 1.40
Hydrophobic (other)			
Proline	heterocyclic	2.03 ± 0.38	12.97 ± 2.44
Phenylalanine	aromatic	-0.96 ± 0.18	-8.81 ± 1.69
Methionine	sulfur	0.51 ± 0.32	4.25 ± 2.64
Hydrophilic (polar)			
Cysteine	sulfur	-0.10 ± 0.21	-0.69 ± 1.40
Serine	hydroxyl	-2.08 ± 0.14	-12.13 ± 0.79
Threonine	hydroxyl	-0.90 ± 0.37	-5.95 ± 2.44
Asparagine	amide	-2.04 ± 0.31	-14.99 ± 2.28
Glutamine	amide	-1.14 ± 0.15	-9.26 ± 1.19
Histidine	heterocyclic	-1.33 ± 0.09	-11.50 ± 0.79
Hydrophilic (ionic)			
Lysine	basic	-2.72 ± 0.47	-22.09 ± 3.84
Arginine	basic	-4.31 ± 0.99	-41.70 ± 9.57
Peptides			
Glycine	polyglycine	-1.01 ± 0.19	-4.22 ± 0.81
Diglycine	polyglycine	-1.45 ± 0.27	-10.68 ± 1.96
Triglycine	polyglycine	-2.58 ± 0.14	-27.11 ± 1.50
Alanine	polyalanine	1.10 ± 0.36	5.47 ± 1.78
Dialanine	polyalanine	0.82 ± 0.18	7.30 ± 1.61
Trialanine	polyalanine	1.44 ± 0.40	18.54 ± 5.13

The I-value is the experimentally measured deviation from ideal in units of (mass of water per mass of solute). The I_n-value is calculated by converting the units to (molecules of water per molecule of solute). I_n-values are useful in visualizing the water perturbation per solute particle, and they allow the correlation of that perturbation with particle molecular characteristics.

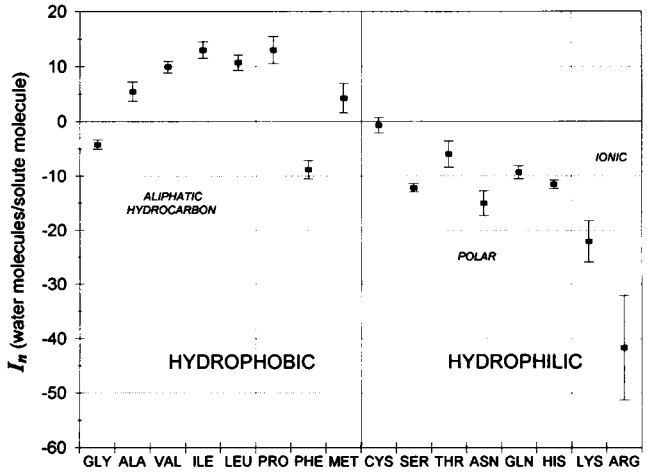

FIGURE 4 Plot of the I_n-values of 16 water-soluble amino acids with 95% confidence intervals. The x axis indicates solute identity with solute molecules grouped by side-chain characteristics. I_n-values measure nonideality in terms of perturbed water molecules per solute molecule.

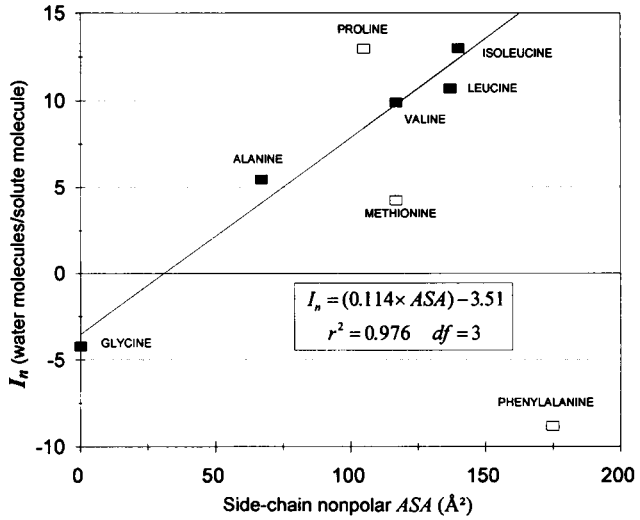

FIGURE 5 Plot of I_n-values versus nonpolar, solvent-accessible, side-chain surface area (ASA) of hydrophobic amino acids as calculated by Miller et al. (1987). The regression line is for the five solutes with aliphatic, noncyclic hydrocarbon side-chains (■) that differ from each other in hydrophobic surface area only, leading to changes in the amount of water structuring per solute molecule. The deviations from this regression relationship for the nonaliphatic residues (□) are attributed to their specific molecular characteristics that lead to changes in the amount of water destructuring as well as water structuring.

DISCUSSION

I_n-values, instead of I-values, are used in this discussion because I_n-values allow the correlation of nonideality with particle properties. Statistical analysis was also performed on I_n-values. Each of the following groups was analyzed with one-way ANOVA and found to contain highly significant ($p \ll 0.001$) differences in I_n: all amino acids; all hydrophobics; aliphatic hydrophobics; hydrophilic polar; peptides of glycine; peptides of alanine. Each of the above groups was then analyzed with the SNK multiple range test for differences at the $p = 0.05$ level of significance. Each of the eight hydrophobics is different from at least six others in that group; all of the hydrophilics are significantly different from each other (except for histidine, which is not significantly different from serine). The three peptides of glycine are significantly different from each other; trialanine is significantly different from the other two peptides of alanine.

Hydrophobic surface area: solvent structuring

Structure occurs in bulk water because of positional restrictions caused by multiple hydrogen bonds between adjacent water molecules. This structuring increases adjacent to hydrophobic surfaces because of reduced rotational freedom and translational motion of adjacent water molecules. Structuring increases the number and duration of hydrogen bonds between adjacent water molecules. Increased structuring causes a positive deviation from ideal and is measured with a positive I-value; the magnitude of the I-value increases to reflect the magnitude of increased structuring.

Increased water structuring is observed with all of the hydrophobic amino acids tested except for glycine and phenylalanine. In Fig. 5, the measured I_n-value is plotted against the nonpolar solvent-accessible surface area (ASA) of the amino acid side-chain (Table 1) calculated by S. Miller using the rolling ball method (Miller et al., 1987). Regression analysis was performed on the data for the five hydrophobic amino acids with aliphatic hydrocarbon side chains. These have identical base chains containing identical hydrophilic surfaces and charge geometries. Therefore, these five amino acids differ only in the nonpolar ASA of their side chains. The linear regression line fit for these data yields the equation

$$I_n = (0.114 \times \text{side-chain } ASA) - 3.51, \qquad (10)$$

which has a correlation coefficient of $r = 0.988$ with 3 degrees of freedom. The inverse of the slope shows that water structuring increases at the rate of one perturbed water molecule per 8.8 Å^2 of hydrophobic surface area. This implies that approximately one layer of perturbed water surrounds hydrophobic surface areas, because the surface area occupied by a water molecule is approximately 9.6 Å^2. The intercept of -3.51 is due to destructuring caused by the electric dipole of the base chain as described next.

Solute dipole strength: solvent destructuring

The hydrophilic amino acids, as well as phenylalanine and peptides of glycine, have negative deviations from ideal. We attribute this to a decrease in water structuring in the volume adjacent to polar surfaces because of dielectric alignment as described by Debye-Hückel (Debye and Hückel, 1923; Robbins, 1972). Dielectric realignment results in increased rotational and translational motion of the water molecules and fewer hydrogen

bonds (Fig. 6). The destructuring due to polar surfaces, $I_n^{(polar)}$, may be calculated by subtracting the structuring due to hydrophobic surfaces, $I_n^{(nonpolar)}$, from the I_n-value:

$$I_n^{(nonpolar)} = 0.114 \times ASA^{(side\text{-}chain\ nonpolar)} \quad (11)$$

$$I_n^{(polar)} = I_n - I_n^{(nonpolar)}. \quad (12)$$

The destructuring for all 20 solutes is plotted in Fig. 7. The constant separation of charges in the amino-carboxyl dipole of the single-residue amino acids causes a constant amount of destructuring due to the base chain: $I_n = -3.51$ perturbed water molecules per amino acid molecule, approximately the destructuring measured with glycine ($I_n = -4.22$), which is essentially a base chain with no side chain. Increasing the length of the glycine peptide moves the positive and negative ions of the zwitterion further apart, thus increasing the electric dipole strength (Fig. 8) and increasing the destructuring. Because the side-chain *ASA* of glycine is zero (Miller et al., 1987), the hydrophobic surface area does not increase as the peptide size is increased from one to three residues. Destructuring increases from $I_n = -4.22$ with glycine to $I_n = -27.11$ with triglycine (Fig. 9). The increased destructuring is also evident when observing the mass of perturbed water per mass of solute: $I = -1.01$ for glycine versus $I = -2.58$ for triglycine (Table 4).

Additivity: summation of structuring and destructuring

Increased structuring and destructuring are competing effects that can be seen with peptides of alanine, in which increasing the number of residues increases both the side-chain *ASA* and the electric dipole strength (Fig. 8). The structuring can be

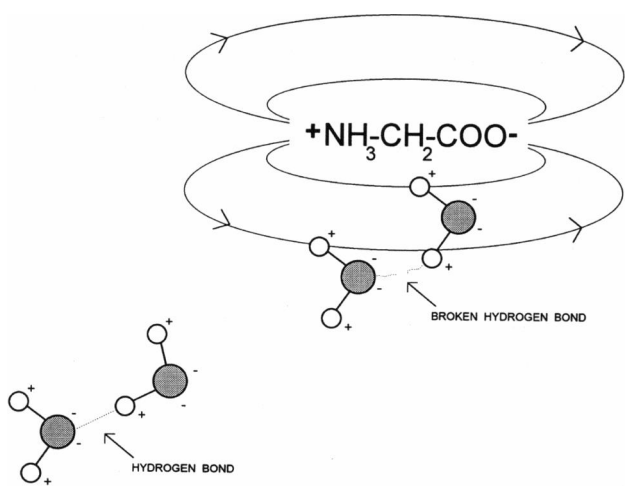

FIGURE 6 Bulk water is characterized by structuring due to multiple hydrogen bonds between adjacent water molecules (*lower left*). An electric field breaks hydrogen bonds by perturbing the orientation of water molecules, thus decreasing water structure (*upper right*).

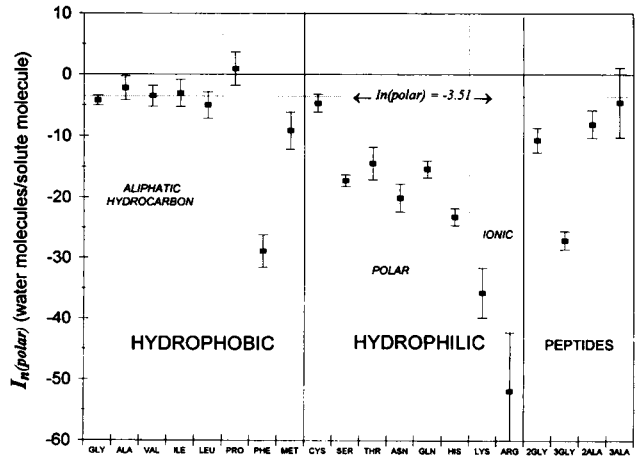

FIGURE 7 The amount of water destructuring per solute molecule is calculated by subtracting the hydrophobic structuring from the measured I_n-value. The aliphatic hydrocarbons are left with $I_n^{(polar)} = -3.51$, the destructuring due to the zwitterion of the base chain. The hydrophilics are more negative because of the additional destructuring due to polar areas of their side-chains.

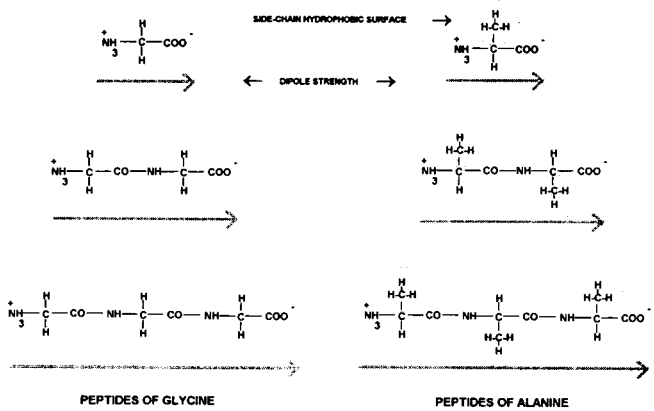

FIGURE 8 Increasing the number of residues in polyglycine increases the dipolar strength by increasing the separation of charges. The side-chain hydrophobic *ASA* remains zero. Increasing the number of residues in polyalanine increases the side-chain hydrophobic *ASA* as well as the dipolar strength. Therefore, polyalanine shows increased water structuring as well as increased water destructuring, the net effect being increased structuring (positive I). Polyglycine has increased destructuring only (negative I).

predicted from Eq. 11, and the destructuring can be predicted from I_n of glycine peptides of equal number of residues. Therefore,

$$I_n^{(2Ala\text{-}predicted)} = 0.114 \times 2ASA^{(Ala)} + I_n^{(2Gly)} = 4.60$$

$$I_n^{(2Ala\text{-}measured)} = 7.30$$

$$I_n^{(3Ala\text{-}predicted)} = 0.114 \times 3ASA^{(Ala)} + I_n^{(3Gly)} = -4.20$$

$$I_n^{(3Ala\text{-}measured)} = 18.54.$$

The net effect is more structuring than the simple summation of the hydrophobic structuring and electric dipole destructuring. We hypothesize that this is because the alanine

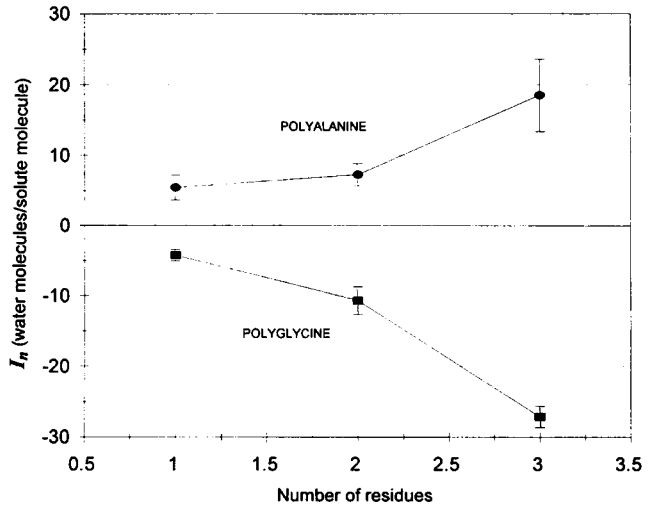

FIGURE 9 Water structuring and destructuring around homopeptides. Polyglycine shows an increased negative deviation from ideal as the number of residues increases. Polyalanine shows an increased positive deviation from ideal as the number of residues increases.

TABLE 5 Comparison of amino acid pairs with similar molecular characteristics

	Side-chain hydrophobic *ASA* (Å^2)	I_n
Sulfur-containing		
Cysteine	35	−0.69
Methionine	117	4.25
Amide-containing		
Asparagine	44	−14.99
Glutamine	53	−9.26
Hydroxyl-containing		
Serine	44	−12.13
Threonine	74	−5.95
Similar molecular weight		
Threonine (A = 119.1)	74	−5.95
Valine (A = 117.1)	117	9.91

In each of the first three pairs, both of the amino acids have identical bases and nearly identical side-chain polar characteristics: they differ in side-chain hydrophobic *ASA* only. The last pair differ in side-chain polar characteristics as well as side-chain hydrophobic *ASA*. In each case, increasing the hydrophobic *ASA* increases I_n, indicating an increase in water structuring even though the net effect may be destructuring.

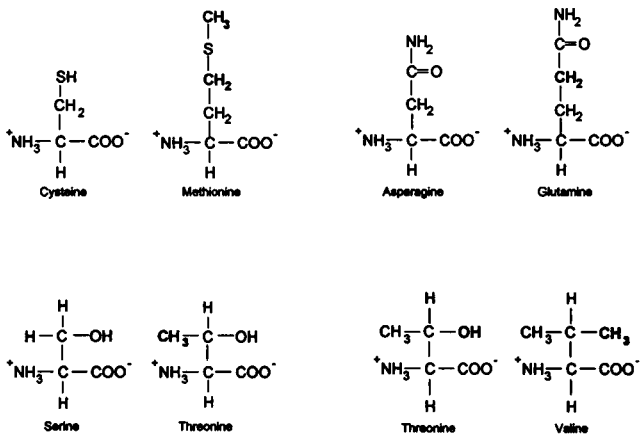

FIGURE 10 Comparison of amino acid pairs with similar molecular characteristics. Cysteine and methionine are both sulfur-containing. Asparagine and glutamine are both amide-containing. Serine and threonine are both hydroxyl-containing. Threonine and valine have nearly identical molecular weights and differ only in replacement of the polar hydroxyl group in threonine with a nonpolar methyl group in valine. A comparison of the side-chain hydrophobic *ASA* and I_n-value for each pair is shown in Table 5.

side chains occupy the volume adjacent to the base chain where the electric field is the strongest; this volume is no longer accessible to solvent destructuring.

The competing effects of structuring and destructuring explain the deviations from the hydrophobic *ASA* regression relationship (Eq. 10) seen with phenylalanine, proline, and methionine (Fig. 5). Phenylalanine's benzene ring has local separations of positive and negative charges between the aromatic-ring hydrogens and the electron-rich π cloud (Thomas et al., 1982). Although the benzene ring has no net electric dipole, phenylalanine exhibits increased destructuring due to these local dipoles and, therefore, causes less structuring than would be predicted based on increased hydrophobic surface area. Proline, an imino acid, has a hydrophobic, nonaromatic ring incorporating part of its base, thus reducing the base-chain *ASA* (Miller et al., 1987) and reducing the base-chain destructuring, which is constant in the other 15 amino acids. Therefore, proline causes more net structuring than would be predicted based on its hydrophobic surface area and base-chain dipole. Methionine has a polar sulfur molecule in its side-chain that adds an additional structure-breaking dipole, thus causing less net structuring than would be predicted based only on its hydrophobic surface area and base-chain dipole.

A similar combination of structuring and destructuring summation occurs with the hydrophilic amino acids, although the net effect is increased water destructuring. Table 5 and Fig. 10 show four pairs of amino acids; each pair consists of two molecules that share many molecular similarities but have one notable difference. All of the pairs confirm that increasing the hydrophobic surface area increases structuring (increasing I-value) whereas increasing polarity decreases structuring (decreasing I-value). Hydrophilic cysteine and hydrophobic methionine contain a polar, structure-breaking sulfur. Cysteine causes net water destructuring ($I_n = -0.69$), whereas methionine, because of its greater hydrophobic surface area, causes net water structuring ($I_n = +4.25$). Asparagine and glutamine have side chains ending with a polar, structure-breaking amide group. Asparagine ($I_n = -14.99$), with the smaller hydrophobic surface area, causes more net water destructuring than glutamine ($I_n = -9.26$). Threonine and serine have side chains containing a polar, structure-breaking hydroxyl group. Serine ($I_n = -12.13$), with the smaller hydrophobic surface area, causes more net destructuring than threonine ($I_n = -5.95$). These differences in I_n-values were previously shown to be significant.

The final comparison is hydrophilic threonine with hydrophobic valine. They have identical base chains and nearly identical molecular weights (119.1 vs. 117.1). The two molecules differ only by a structure-breaking, polar hydroxyl group in threonine versus a structure-making, hydrophobic methyl group in valine. This relative decrease in hydrophobic surface area accompanied with the additional dipole explains the net water destructuring associated with threonine ($I_n = -5.95$) versus the net water structuring associated with valine ($I_n = +9.91$). Although solute volume occupancy could explain the positive deviation from ideal seen with valine (Minton, 1983b), it cannot explain the corresponding negative deviation from ideal seen with threonine, because both molecules have nearly identical volumes.

Intercomparison of I_n-values and hydrophobicity scales

We compared our scale of amino acid I_n-values with eight hydrophobicity scales from the literature. These scales and their coefficients of correlation are shown in Table 6. Fig. 11 shows a plot of the free energy of transfer from vapor to water (Radzicka and Wolfenden, 1988) versus the I_n-values presented in this paper. The correlation is highly significant ($p < 0.01$ with $r = 0.91$ and 13 degrees of freedom). The correlation with I_n is significant ($p < 0.05$) for all of the hydrophobicity scales and highly significant ($p < 0.01$) for seven of them. The importance of polar characteristics in our I_n nonideality scale and the high degree of correlation between our scale and the other "hydrophobicity" scales confirm the importance of hydrophilic as well as hydrophobic surface effects in determining free energies of transfer of solutes from hydrophobic to hydrophilic solvents (Ben-Naim, 1990).

SUMMARY AND CONCLUSIONS

These experiments on the freezing-point depression of amino acid solutions confirm that the nonideality constant I in the interaction-corrected expression is due to the solvent

TABLE 6 Correlation of I_n-values with "hydrophobicity" scales from the literature

Amino acid	(a) I_n	(b) Cyclohexane-water	(c) Vapor-water	(d) Octane-water	(e) Aboderin	(f) Chothia	(g) Guy	(h) Black	(i) Bull-Breeze
Arginine	−41.70	−14.92	−19.92	−1.32	2.0	−2.71	−0.84	0.000	−0.69
Lysine	−22.09	−5.55	−9.52	0.08	1.3	−2.05	−1.18	0.283	−0.46
Asparagine	−14.99	−6.64	−9.68	−0.01	0.6	−1.18	−0.48		−0.89
Serine	−12.13	−3.40	−5.06	0.04	3.1	−0.75	−0.50	0.359	−0.42
Histidine	−11.50	−4.66	−10.27	0.95	1.6	−0.94	0.49	0.165	−0.69
Glutamine	−9.26	−5.54	−9.38	−0.07	1.4	−1.53	−0.73	0.251	−0.97
Phenylalanine	−8.81	2.98	−0.76	2.09	9.6	0.00	1.27	1.000	1.52
Threonine	−5.95	−2.57	−4.88	0.27	3.5	−0.71	−0.27	0.450	−0.29
Glycine	−4.22	0.94	2.39	0.00	4.1	−0.34	−0.41	0.501	−0.81
Cysteine	−0.69	1.28	−1.24			0.00	1.36	0.680	−0.36
Methionine	4.25	2.35	−1.48	1.32	8.7	−0.24	1.27	0.236	0.66
Alanine	5.47	1.81	1.94	0.52	5.1	−0.29	−0.06	0.616	−0.61
Valine	9.91	4.04	1.99	1.18	8.5	0.09	1.09	0.825	0.75
Leucine	10.70	4.92	2.28	1.76	10.0	0.24	1.31	0.738	1.65
Isoleucine	12.98	4.92	2.15	2.04	9.3	−0.12	1.21	0.943	1.45
Proline	12.97				4.9			0.711	0.17
Glutamic acid		−6.81	−10.24	−0.79	1.8	−0.90	−0.77	0.043	−0.51
Tyrosine		−0.14	−6.11	1.63	8.0	−1.02	0.33	0.880	1.43
Tryptophan		2.33	−5.88	2.51	9.2	−0.59	0.88	0.878	1.20
Aspartic acid		−8.72	−10.95		0.7	−1.02	−0.80	0.028	−0.61

Correlation (j)	I_n	Significance	Cyclohexane-water	Vapor-water	Octane-water	Aboderin	Chothia	Guy	Black	Bull-Breeze
I_n	1.00									
Cyclohexane-water	0.94	0.01	1.00							
Vapor-water	0.91	0.01	0.94	1.00						
Octane-water	0.77	0.01	0.84	0.61	1.00					
Aboderin	0.68	0.01	0.86	0.71	0.86	1.00				
Chothia	0.90	0.01	0.89	0.90	0.68	0.71	1.00			
Guy	0.71	0.01	0.81	0.66	0.88	0.90	0.78	1.00		
Black	0.71	0.01	0.84	0.72	0.83	0.84	0.65	0.71	1.00	
Bull-Breeze	0.56	0.05	0.70	0.50	0.86	0.93	0.54	0.76	0.77	1.00

(a) Experimentally measured solution nonideality in terms of perturbed water molecules per solute molecule. (b) Measured free energies of transfer (kcal/mol) from dilute solution of cyclohexane to dilute aqueous solution (Radzicka and Wolfenden, 1988). (c) Measured free energies of transfer (kcal/mol) from vapor phase to neutral aqueous (Radzicka and Wolfenden, 1988). (d) Measured free energies of transfer (kcal/mol) from octanol to neutral aqueous solution (Radzicka and Wolfenden, 1988). (e) Measured relative mobilities of amino acids on chromatographic paper (Aboderin, 1971). (f) Calculated virtual free energy of transfer of residues from outside to inside of a sample of certain proteins, based on the fraction of the total number of residues that are 95% buried in the native structure of the protein (Chothia, 1976). (g) Mean polarity calculated from layer analysis of distributions of residues in proteins (Guy, 1985). (h) Logarithm of partition coefficient for transfer from polar to nonpolar phase (Black and Mould, 1991). (i) Free energies of transfer of amino acid residues from surface to solution calculated from surface tensions of amino acids in 0.10 M NaCl (Bull and Breeze, 1974). (j) Linear correlation coefficient of the horizontal row with the vertical row. The third column shows the significance of the correlation of each "hydrophobicity" scale with the I_n nonideality scale.

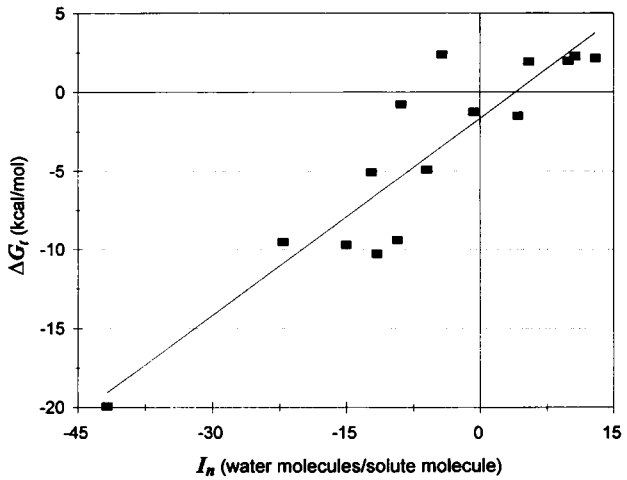

FIGURE 11 Plot of Radzicka and Wolfenden's vapor-to-water hydrophobicity scale (free energies of transfer in kcal/mol) versus I_n-value (solution nonideality in perturbed water molecules per solute molecule) of the 15 soluble amino acids common to both scales. The correlation coefficient of $r = 0.91$ is highly significant ($p < 0.01$).

structuring/destructuring influences of the solute on the solvent. Positive *I*-values indicate water structuring adjacent to hydrophobic surface areas consistent with a single monolayer of water as predicted by others (Marchesi, 1983; Rossky and Karplus, 1979; Sonnenschein and Heinzinger, 1983; Zubay, 1983). Negative *I*-values indicate destructuring due to interactions of the water dipole with the relatively immobile electric field induced by the solute. The *I*-value of a specific solute reflects the summation of both structuring and destructuring influences based on molecular characteristics including hydrophobic surface area, electric dipole strength, and distribution, and the solvent-accessible volume. The high degree of correlation between I_n-values and a variety of "hydrophobicity" scales confirms that both hydrophilic and hydrophobic surface effects are crucial in determining the free energy of transfer of solutes from hydrophobic to hydrophilic solvents. The capacity to predict hydrophilic influences on the basis of molecular characteristics will require careful characterization of *I*-values as a function of charge, charge distribution, and solute geometry for a range of solute molecules.

REFERENCES

Aboderin, A. 1971. An empirical hydrophobicity scale for α-amino-acids and some of its applications. *Int. J. Biochem.* 2:537–544.

Arakawa, T., R. Bhat, and S. N. Timasheff. 1990a. Preferential interactions determine protein stability in three-component solutions: the $MgCl_2$ system. *Biochemistry.* 29:1914–1923.

Arakawa, T., R. Bhat, and S. N. Timasheff. 1990b. Why preferential hydration does not always stabilize the native structure of globular proteins. *Biochemistry.* 29:1924–1931.

Arakawa, T., and S. N. Timasheff. 1984. Mechanism of protein salting in and salting out by divalent salts: balance between hydration and salt binding. *Biochemistry.* 23:5912–5923.

Ben-Naim, A. 1990. Solvent effects on protein association and protein folding. *Biopolymers.* 29:567–596.

Black, S., and D. Mould. 1991. Development of hydrophobicity parameters to analyze proteins which bear post- or cotranslational modifications. *Anal. Biochem.* 193:72–82.

Bull, H., and K. Breeze. 1974. Surface tension of amino acid solutions: a hydrophobicity scale of the amino acid residues. *Arch. Biochem. Biophys.* 161:665–670.

Chothia, C. 1976. The nature of the accessible and buried surfaces in proteins. *J. Mol. Biol.* 105:1–12.

Debye, P., and E. Huckel. 1923. The theory of electrolytes. I. Lowering of freezing point and related phenomena. *Physik Z.* 24:185–206.

DeRobertis, E. D. P., and E. M. F. DeRobertis. 1980. Molecular components and metabolism of the cell. *In* Cell and Molecular Biology. Holt, Rinehart and Winston, Philadelphia, PA. 69–114.

Enderby, J. E., and G. W. Neilson. 1980. Structural properties of ionic liquids. *Adv. Phys.* 29:323*a*. (Abstr.)

Enderby, J. E., and G. W. Neilson. 1981. The structure of electrolyte solutions. *Rep. Prog. Phys.* 44:593–653.

Finney, J. L., and J. Turner. 1986. Neutron diffraction studies of aqueous solutions of molecules of biological importance: an approach to liquid-state structural chemistry. *Ann. N.Y. Acad. Sci.* 402:127–141.

Fullerton, G., C. Keener, and I. Cameron. 1994. Correction for solute/solvent interaction extends accurate freezing-point depression theory to high concentration range. *J. Biochem. Biophys. Methods.* In press.

Fullerton, G. D., V. A. Ord, and I. L. Cameron. 1986. An evaluation of the hydration of lysozyme by an NMR titration method. *Biochem. Biophys. Acta.* 869:230–246.

Fullerton, G., R. J. Zimmerman, C. Cantu, and I. Cameron. 1992. New expressions to describe solution nonideality: osmotic pressure, freezing-point depression and vapor pressure. *Biochem. Cell. Biol.* 70:1325–1331.

Fullerton, G. D., R. J. Zimmerman, K. M. Kanal, J. Floyd, and I. L. Cameron. 1993. Methods to improve the accuracy of membrane osmometry measures of protein molecular weight. *J. Biochem. Biophys. Methods.* 20:299–307.

Geiger, A. 1981. Molecular dynamics simulation study of the negative hydration effect in aqueous electrolyte solutions. *Ber. Bunsenges. Phys. Chem.* 85:52–63.

Grosch, L., and F. Noack. 1976. NMR relaxation investigation of water mobility in aqueous bovine serum albumin solutions. *Biochem. Biophys. Acta.* 453:218–232.

Guy, H. R. 1985. Amino acid side-chain partition energies and distribution of residues in soluble proteins. *Biophys. J.* 47:61–70.

Harned, H. S., and B. B. Owen. 1950. The Physical Chemistry of Electrolytic Solutions. Reinhold Publishing, New York.

Hertz, H. G. 1973. Nuclear magnetic relaxation spectroscopy. *In* Water, A comprehensive treatise, Vol. 3. Plenum Press, New York. 301–399.

Kanal, K. M., G. D. Fullerton, and I. L. Cameron. 1994. A study of the molecular sources of nonideal osmotic pressure of bovine serum albumin solutions as a function of pH. *Biophys. J.* 66:153–160.

LeNeveu, D. M., R. P. Rand, and V. A. Parsegian. 1976. Measurement of force between lecithin bilayers. *Nature.* 259:601–603.

LeNeveu, D. M., R. P. Rand, V. A. Parsegian, and D. Gingell. 1977. Measurement and modification of forces between lecithin bilayers. *Biophys. J.* 18:209–230.

Levine, I. N. 1988. Physical Chemistry. McGraw-Hill Book Co., New York. 260–296.

Marchesi, M. 1983. Molecular dynamics simulation of liquid water between two walls. *Chem. Phys. Lett.* 102:550–554.

Marlow, G. E., J. S. Perkyns, and B. M. Pettit. 1993. Salt effects in peptide solutions: theory and simulation. *Chem. Rev.* 93:2503–2521.

Miller, S., J. Janin, A. M. Lesk, and C. Chothia. 1987. Interior and surface of monomeric proteins. *J. Mol. Biol.* 196:641–656.

Minton, A. P. 1983a. The effect of volume occupancy upon the thermodynamic activity of proteins: some biochemical consequences. *Mol. Cell. Biochem.* 55:119–140.

Minton, A. P. 1983b. Thermodynamic nonideality and the dependence of partition coefficient upon solute concentration upon solute concentration in exclusion chromatography. II. An improved theory of equilibrium partitioning of concentration protein solutions. Application to hemoglobin. *Biophys. Chem.* 18:139–143.

Minton, A. P., and H. Edelhoch. 1982. Light scattering of bovine serum albumin solutions: extension of the hard particle model to allow for electrostatic repulsion. *Biopolymers.* 21:451–458.

Parsegian, V. A. 1967. Forces between lecithin bimolecular leaflets are due to a disordered surface layer. *Science.* 156:939–942.

Parsegian, V. A., R. P. Rand, N. L. Fuller, and D. C. Rau. 1986. Osmotic stress for the direct measurement of intermolecular forces. *In* Methods in Enzymology 127: Biomembranes Part O (Protons and Water: Structure and Translocation). Academic Press, Orlando, FL. 400–416.

Prouty, M. S., A. N. Schechter, and V. A. Parsegian. 1985. Chemical potential measurements of deoxyhemoglobin s polymerization, determination of the phase diagram of an assembling protein. *J. Mol. Biol.* 184:517–528.

Radzicka, A., and R. Wolfenden. 1988. Comparing the polarities of the amino acids: side-chain distribution coefficients between the vapor phase, cyclohexane, 1-octanol, and neutral aqueous solution. *Biochemistry.* 27: 1664–1670.

Robbins, J. 1972. Ions in Solution (2), An Introduction to Electrochemistry. Clarendon Press, Oxford. 1–15.

Rossky, P. J., and M. Karplus. 1979. Solvation. A molecular dynamics study of a dipeptide in water. *J. Am. Chem. Soc.* 101:1913–1937.

Sonnenschein, R., and K. Heinzinger. 1983. A molecular dynamics study of water between Lennard-Jones walls. *Chem. Phys. Lett.* 102:550–554.

Soper, A. K., G. W. Neilson, J. E. Enderby, and R. A. Howe. 1977. Neutron diffraction study of hydration effects in aqueous solutions. *J. Phys. Chem.* 10:1793–1801.

Streitweiser, A., and C. Heathcock. 1981. Amino acids, peptides, and proteins. *In* Introduction to Organic Chemistry. Macmillan, New York. 935–981.

Thomas, K., G. Smith, T. Thomas, and R. Feldmann. 1982. Electronic distributions within protein phenylalanine rings are reflected by the three-dimensional oxygen atom environments. *Proc. Natl. Acad. Sci. USA.* 79:4843–4847.

Weast, R. 1981. Physical constants of organic chemicals. *In* CRC Handbook of Chemistry and Physics. CRC Press, Boca Raton, FL. C51–C576.

Zimmerman, R., H. Chao, G. Fullerton, and I. Cameron. 1993. Solute/solvent interaction corrections account for non-ideal freezing point depression. *J. Biochem. Biophys. Methods.* 26:61–70.

Zimmerman, S., A. Zimmerman, G. Fullerton, R. Luduena, and I. Cameron. 1985. Water ordering during the cell cycle: Nuclear Magnetic Resonance studies of the sea-urchin egg. *J. Cell Sci.* 79:247–257.

Zubay, G. 1983. Anatomy of protein structure. *In* Biochemistry. Addison-Wesley, Reading, MA. 68–129.